Yttrium Complexes of a Phenanthrene-Fused Cyclopentadienyl: Synthetic, Structural, and Reactivity Studies

Jianlong Sun, David J. Berg,* and Brendan Twamley†

Department of Chemistry, University of Victoria, P.O. Box 3065, Victoria, British Columbia, Canada V8W 3V6

Received July 20, 2007

The tris-alkyl complex $Y(CH_2SiMe_3)_3(THF)_2$ reacts with 1,2,3-trimethyl-1*H*-cyclopenta[*l*]phenanthrene (PCp*H) to give (PCp*)$Y(CH_2SiMe_3)_2$(THF) (**1**), characterized structurally by X-ray crystallography. VT NMR spectra of **1** reveal a dynamic equilibrium between the THF-free and mono(THF) solvate in solution. Complex **1** undergoes substitution of THF by 2,2′-bipyridine (bipy) to give (PCp*)-$Y(CH_2SiMe_3)_2$(bipy) (**2**); the latter complex does not undergo ligand exchange in solution. Insertion reactions of **1** with CO_2, Me_3SiNCO, and $Me_2CHN{=}C{=}NCHMe_2$ afford (PCp*)$Y[\kappa^2$-(O,O)-$O_2C(CH_2SiMe_3)]_2$ (**3**), (PCp*)$Y[\kappa^2$-(N,O)-$(Me_3Si)NC(CH_2SiMe_3)O]_2$ (**4**), and (PCp*)$Y[\kappa^2$-(N,N)-$(Me_2CH)NC(CH_2SiMe_3)N(CHMe_2)]_2$ (**5**). Reaction of **1** with 2 equiv of Me_3SiCCH affords a terminal bis(acetylide) (PCp*)$Y(CCSiMe_3)_2$(THF) (**6**) in solution; however, X-ray analysis of crystals obtained from a solution of **6** shows that it dimerizes to $\{[(PCp^*)Y(CCSiMe_3)(THF)]_2(\mu$-$CCSiMe_3)_2\}$ (**7**). A toluene solution of complex **1** and 1 equiv of $[Ph_3C]^+[B(C_6F_5)_4]^-$ shows modest catalytic activity for the polymerization of ethylene at room temperature (20 kg mol^{-1} $h^{-1}bar^{-1}$).

Introduction

Cyclopentadienyl complexes of yttrium and the lanthanoids have been extensively studied over the past 30 years and constitute the best known class of ancillary ligand in the organometallic chemistry of these elements.[1] In the development of this chemistry, pentamethylcyclopentadienyl, bis(trimethylsilyl)cyclopentadienyl, and other alkyl-substituted Cp ligands have been most extensively used because their increased bulk allows isolation of soluble, monomeric or dimeric complexes free from extensive bridging interactions that plague Cp and its smaller analogues.[2] While this strategy has obvious merit, excessive ancillary ligand bulk is usually detrimental to reactivity at any remaining metal–carbon bonds because the alkyl substituents block reactant access;[3] in the case of bent metallocenes, this is clearly because the substituents on the Cp ligands project into the metallocene wedge. One possible solution to this problem is to incorporate planar bulk on the Cp ligand so that bridging interactions between adjacent metal centers are disrupted, but access within the metallocene wedge is still relatively unimpeded.

Indenyl and fluorenyl complexes represent the simplest implementation of this idea, and many complexes of these ligands are known.[4] Surprisingly, larger aromatic-fused cyclopentadienyl ligands have not received very much attention in yttrium or lanthanoid chemistry, although a few examples have been reported for the group 4 metals.[5] One criticism of this approach might be that extensive delocalization of charge within the extended aromatic system weakens the bonding between the metal and the Cp unit since this bonding is primarily ionic in nature. However, calculations on the phenanthrene-fused (PCp) or bis(phenanthrene)-fused (sCp) anions indicate that the reduction in charge on the five carbons of the Cp subunit caused by fusion of two (PCp) or four (sCp) additional benzene units

* Corresponding author. E-mail: djberg@uvic.ca.
† University Research Office, 109 Morrill Hall, University of Idaho, Moscow ID 83844-3010.

(1) (a) Edelmann, F. T.; Lorenz, V. *Coord. Chem. Rev.* **2000**, *209*, 99. (b) Schumann, H.; Meese-Marktscheffel, J. A.; Esser, L. *Chem. Rev.* **1995**, *95*, 865. (c) Schaverien, C. J. *Adv. Organomet. Chem.* **1994**, *36*, 283.

(2) (a) Evans, W. J.; Anwander, R.; Doedens, R. J.; Ziller, J. W. *Angew. Chem., Int. Ed. Engl.* **1994**, *33*, 1641. (b) Arndt, S.; Okuda, J. *Chem. Rev.* **2002**, *102*, 1953. (c) van der Heijden, H.; Schaverien, C. J.; Orpen, A. G. *Organometallics* **1989**, *8*, 255. (d) Heeres, H. J.; Meetsma, A.; Teuben, J. H.; Rogers, R. D. *Organometallics* **1989**, *8*, 2637.

(3) (a) The exception to this rule is the remarkable chemistry uncovered by Evans for "sterically oversaturated" $Ln(C_5Me_5)_3$ systems; see for example: Evans, W. J.; Kozimor, S. A.; Ziller, J. W. *Inorg. Chem.* **2005**, *44*, 7960. (b) Evans, W. J.; Perotti, J. M.; Kozimor, S. A.; Champagne, T. M.; Davis, B. L.; Nyce, G. W.; Fujimoto, C. H.; Clark, R. D.; Johnston, M. A.; Ziller, J. W. *Organometallics* **2005**, *24*, 3916.

(4) (a) A complete list of all yttrium and lanthanoid indenyl and fluorenyl systems is too extensive to give here; recent examples, many containing pendant functionality, are given below: Zhou, S.; Wang, S.; Yang, G.; Li, Q.; Zhang, L.; Yao, Z.; Zhou, Z.; Song, H. *Organometallics* **2007**, *26*, 3755. (b) Downing, S. P.; Conde Guadaño, S.; Pugh, D.; Danopoulos, A. A.; Bellabarba, R. M.; Hanton, M.; Smith, D.; Tooze, R. P. *Organometallics* **2007**, *26*, 3762. (c) Wang, B.; Wang, D.; Cui, D.; Gao, W.; Tang, T.; Chen, X.; Jing, X. *Organometallics* **2007**, *26*, 3167. (d) Trifonov, A. A.; Federova, E. A.; Borovkov, I. A.; Fukin, G. K.; Baranov, E. V.; Larionova, J.; Druzhkov, N. O. *Organometallics* **2007**, *26*, 2488. (e) Wang, S.; Tang, X.; Vega, A.; Saillard, J.-Y.; Zhou, S.; Yang, G.; Yao, W.; Wei, Y. *Organometallics* **2007**, *26*, 1512. (f) Lewin, J. L.; Woodrum, N. L.; Cramer, C. J. *Organometallics* **2006**, *25*, 5906. (g) Pi, C.; Zhang, Z.; Liu, R.; Weng, L.; Chen, Z.; Zhou, X. *Organometallics* **2006**, *25*, 5165. (h) Wang, S.; Tang, X.; Vega, A.; Saillard, J.-Y.; Sheng, E.; Yang, G.; Zhou, S.; Huang, Z. *Organometallics* **2006**, *25*, 2399. (i) Shen, H.; Chan, H.-S.; Xie, Z. *Organometallics* **2006**, *25*, 2617.

(5) (a) To the best of our knowledge, there are no structurally characterized examples of aromatic-fused cyclopentadienyls (excluding fullerene systems) larger than fluorenyl for yttrium or the lanthanoids; examples from group 4 are as follows: Spaleck, W.; Kuber, F.; Winter, A.; Rohrmann, J.; Bachmann, B.; Antberg, M.; Dolle, V.; Paulus, E. F. *Organometallics* **1994**, *13*, 954. (b) Stehling, U.; Diebold, J.; Kirsten, R.; Röll, W.; Brintzinger, H. H.; Jüngling, S.; Mülhaupt, R.; Langhauser, F. *Organometallics* **1994**, *13*, 964. (c) Schneider, N.; Huttenloch, M. E.; Stehling, U.; Kirsten, R.; Schaper, F.; Brintzinger, H. H. *Organometallics* **1997**, *16*, 3413. (d) Schneider, N.; Prosenc, M. H.; Brintzinger, H. H. *J. Organomet. Chem.* **1997**, *545–546*, 291. (e) Schneider, N.; Schaper, F.; Schmidt, K.; Kirsten, R.; Geyer, A.; Brintzinger, H. H. *Organometallics* **2000**, *19*, 3597.

10.1021/om7007343 CCC: $40.75
Publication on Web 01/19/2008

to the indenyl or fluorenyl core, respectively, is very small.[6,7] The greatest reduction in charge on the Cp occurs when the benzene unit is fused directly to the Cp as in indenyl or fluorenyl themselves, while more remote fusion has relatively little effect.[7] Therefore, inasmuch as indenyl and fluorenyl complexes of yttrium and the lanthanoids are stable, there is no reason *a priori* to expect weak metal–ligand bonding to dominate larger systems because the Cp is effectively isolated electronically from these remote aromatic groups. However, it should be noted that a large conjugated aromatic system fused to a Cp might have redox chemistry of its own that becomes significant for metals with multiple oxidation states.[7]

In this contribution we report the synthesis of yttrium complexes containing a phenanthrene-fused Cp bearing three methyl groups on the remaining Cp carbons (PCp*). This is a relatively bulky ligand so it is not surprising that stable mono(PCp*) complexes that show no tendency to redistribute dominate this chemistry. The synthesis of a PCp* yttrium dialkyl complex, its acid–base reaction with trimethylsilylacetylene, and its insertion chemistry with unsaturated substrates are discussed below.

Experimental Section

General Procedures. All reactions were carried out under a nitrogen atmosphere, with the exclusion of water and oxygen, using glovebox (Braun MB150-GII) or vacuum line techniques. All compounds described below were prepared on NMR tube scale first (except for **3**) followed by preparative scale reactions. ^{1}H NMR data from NMR tube scale reactions and isolated solids from preparative scale reactions matched very well for **1/2** and **4**−**6**; only NMR data from the preparative scale reaction is given in the text. Tetrahydrofuran (THF) and diethyl ether were dried by distillation from sodium benzophenone ketyl under argon immediately prior to use; hexane and toluene were dried and deoxygenated using an MBraun solvent purification system and were stored over activated 4 Å sieves in the glovebox. $Y(CH_2SiMe_3)_3(THF)_2$[8] and 1,2,3-trimethyl-1*H*-cyclopenta[*l*]phenanthrene (PCp*H)[9] were prepared as previously reported. The PCp*H ligand was dried over 4 Å sieves prior to use.

NMR spectra were recorded using a Bruker Avance-500 MHz spectrometer: ^{1}H (500.13 MHz) and ^{13}C (125.8 MHz) unless otherwise specified. All deuterated solvents were dried over activated 4 Å molecular sieves except for d_8-tetrahydrofuran (d_8-THF), which was dried by distillation from sodium benzophenone ketyl under argon and stored over activated 4 Å molecular sieves. The spectra were recorded using 5 mm tubes fitted with a Teflon valve (Brunfeldt) at room temperature unless otherwise specified and were referenced to residual solvent resonances. Melting points were recorded using a Büchi melting point apparatus in sealed capillary tubes and are not corrected. Elemental analyses were performed by Canadian Microanalytical, Delta, BC; co-oxidants (V_2O_5 or PbO_2) were used during combustion of the metal complexes.

(PCp*)Y(CH$_2$SiMe$_3$)$_2$(THF) (1). A 5 mL toluene solution of PCp*H (129 mg, 0.5 mmol) was added to $Y(CH_2SiMe_3)_3(THF)_2$ (250 mg, 0.5 mmol), and the mixture was stirred overnight. Removal of toluene under reduced pressure gave a yellow residue, which was dissolved completely in hexanes and filtered through Celite to give a clear yellow solution. Removal of hexanes afforded 259 mg of a yellow powder. Recrystallization of this yellow powder from hexane afforded 80 mg of **1** as pale yellow prisms. Yield (recrystallized): 20%. Mp: 110 °C (dec). ^{1}H NMR (500 MHz, C_6D_6): δ 8.47 (dd, $^3J_{HH}$ = 8.2 Hz, $^4J_{HH}$ = 0.8 Hz, 2H, *1-arylH*), 8.25 (dd, $^3J_{HH}$ = 8.4 Hz, $^4J_{HH}$ = 1.0 Hz, 2H, *4-arylH*), 7.34 (m, 2H, *2-arylH*), 7.20 (m, 2H, *3-arylH*), 2.78 (s, 6H, Cp*Me*), 2.52 (t, 4H, α-THF CH_2), 2.32 (s, 3H, Cp*Me*), 0.60 (m, 4H, β-THF CH_2), 0.26 (s, 18H, SiMe_3), −0.60 (d, $^2J_{YH}$= 3.2 Hz, 4H, YCH_2). ^{13}C NMR (125.8 MHz, C_6D_6): δ131.73, 129.00, 128.58, 127.70, 124.72, 124.43, 123.94, 118.26, 113.70 (*arylC*), 70.21 24.69 (THF), 37.40 (d, $^1J_{YC}$= 45 Hz, Y-CH_2), 16.30 (CpMe_2), 11.75 (Cp*Me*), 4.76 (SiMe_3). Anal. Calcd for $C_{32}H_{47}OSi_2Y$: C 64.84, H 8.00. Found: C 64.98, H 8.07.

(PCp*)Y(CH$_2$SiMe$_3$)$_2$(bipy) (2). Addition of a solution of 27 mg of 2.2′-bipyridine (0.17 mmol) in 1 mL of toluene to a solution of 100 mg of **1** (0.169 mmol) in 5 mL of toluene resulted in a color change to deep red. After stirring for 5 min, the solvent was removed by vacuum to give a red solid. Repeated washing with hexane and drying under vacuum gave a deep red powder in quantitative yield. ^{1}H NMR (300 MHz, C_6D_6): δ 8.26 (d, $^3J_{HH}$ = 5.2 Hz, 2H, *6-bipy*), 7.94 (dd, $^3J_{HH}$ = 7 Hz, $^4J_{HH}$ = 2.2 Hz, 2H, *1-arylH*), 7.73 (dd, $^3J_{HH}$ = 7 Hz, $^4J_{HH}$ = 2.6 Hz, 2H, *4-arylH*), 7.03–6.91 (m, 4H, *2,3-arylH*), 6.64 (dt, 2H, $^3J_{HH}$ = 7 Hz, *4-bipy*), 6.35 (d, 2H, $^3J_{HH}$ = 8 Hz, *3-bipy*), 6.28 (dd, $^3J_{HH}$ = 6.6 Hz, $^4J_{HH}$ = 2.2 Hz, 2H, *5-bipy*), 2.76 (s, 6H, Cp*Me*), 2.58 (s, 3H, Cp*Me*), 0.29 (s, 18H, SiMe_3), −0.22 (dd, $^2J_{YH}$ = 3.0 Hz, $^3J_{HH}$ = 11 Hz, 2H, YCH_2), −0.45 (dd, $^2J_{YH}$ =3.0 Hz, $^3J_{HH}$ = 11 Hz, 2H, YCH_2); ^{13}C NMR (75.5 MHz, C_6D_6) δ151.70, 138.64, 128.40, 128.08, 126.80, 124.35, 123.92, 123.35, 122.78, 120.47, 113.30 (*arylC*), 32.98 (d, $^1J_{YC}$ = 38.6 Hz, Y-CH_2), 16.44 (CpMe_2), 12.47 (Cp*Me*), 5.27 (SiMe_3). Anal. Calcd for $C_{38}H_{47}N_2Si_2Y$: C 67.43, H 7.01, N 4.14. Found: C 68.05, H 6.91, N 4.00. This sample did not give an obvious melting point below 200 °C but rather darkened steadily on heating.

(PCp*)Y(κ^2-(O,O)-O$_2$CCH$_2$SiMe$_3$)$_2$ (3). An evacuated Schlenk flask was filled with CO_2 gas that had been dried by passage through a column of activated 4 Å sieves. A solution of **1** (50 mg, 0.082 mmol) in 5 mL of hexanes was injected into the flask by syringe. A white precipitate formed immediately. The suspension was allowed to stir overnight and the solvent was removed under reduced pressure. In the glovebox, the precipitate was washed with hexane and dried under reduced pressure to give 30 mg of **3** as a white powder. Yield: 60%. Mp: 234 °C (dec). ^{1}H NMR (C_6D_6, 500 MHz): δ 8.55 (d, $^3J_{HH}$ = 8.1 Hz, 2H, *1-arylH*), 8.43 (d, $^3J_{HH}$ = 7.6 Hz, 2H, *4-arylH*), 7.42 (m, 2H, *2-arylH*), 7.28 (m, 2H, *3-arylH*), 2.72 (s, 6H, Cp*Me*), 2.30 (s, 3H, Cp*Me*), 1.10 (s, 4H, CO_2CH_2), 0.00 (s, 18H, SiMe_3). ^{13}C NMR (125.7 MHz, C_6D_6): δ 185.42 (CO_2), 132.57, 128.68, 128.39, 128.07, 127.05, 125.38, 124.22, 118.80, 114.46 (*arylC*), 29.63 (CO_2CH_2), 15.26 (CpMe_2), 11.53 (Cp*Me*), −0.62 (SiMe_3). Anal. Calcd for $C_{30}H_{39}O_4Si_2Y$: C 59.20, H 6.46. Found: C 60.18, H, 6.29.

(PCp*)Y[κ^2-(N,O)-Me$_3$SiN(CH$_2$SiMe$_3$)CO]$_2$ (4). Me_3SiNCO (6 mg, 0.05 mmol) was added to 6 mg of **1** (0.01 mmol) in 1 mL of toluene solution and allowed to stir for 5 h. Removal of solvent under vacuum afforded an off-white powder. Repeated washing with hexane and drying under vacuum gave a cream powder in quantitative yield. ^{1}H NMR (C_6D_6, 300 MHz): δ 8.58 (d, $^3J_{HH}$ = 8.0 Hz, 2H, *1-aryl H*), 8.42 (d, $^3J_{HH}$ = 8.0 Hz, 2H, *4-aryl H*), 7.45 (t, $^3J_{HH}$ = 7.3 Hz, 2H, *2-aryl H*), 7.32 (t, $^3J_{HH}$ = 7.4 Hz, 2H, *3-aryl H*), 2.79 (s, 6H, Cp*Me*), 2.31 (s, 3H, Cp*Me*), 1.65 (s, 4H, CH_2SiMe_3), 0.06 (s, 18H, $CH_2Si$$Me_3$), −0.05 (s, 18H, NSi$Me_3$). ^{13}C NMR (75.5 MHz, C_6D_6): δ 188.54 (NCO), 129.68, 128.72, 128.40, 127.25, 125.18, 124.33 (*arylC*), 31.40 (CH_2), 15.28

(6) Simple extended Hückel calculations indicate that direct fusion of an aromatic ring to cyclopentadienide has the greatest effect on the charge on the five-membered ring carbons, while remote fusion has substantially less effect: Cp^- (−1.0 charge on the five-membered ring carbons), indenide (−0.84), fluorenide (−0.59), cyclopenta[*l*]phenanthrenide (PCp, −0.78).

(7) A more in-depth theoretical study of aromatic-fused cyclopentadienyls in the gas phase and in solution supports the trend in ref 6 and clearly shows that the position of ring fusion is also important as might be expected. Yoshizawa, K.; Yahara, K.; Taniguchi, A.; Yamabe, T.; Kinoshita, T.; Takeuchi, K. *J. Org. Chem.* **1999**, *64*, 2821.

(8) Barker, F. K.; Lappert, M. F. *J. Organomet. Chem.* **1974**, *76*, C45.

(9) Jones, D. W. J. *Chem. Soc., Perkin Trans. 1* **1977**, 980.

(Cp*Me*$_2$), 11.92 (Cp*Me*), 1.67 (CH_2Si*Me*$_3$), −0.28 (NSi*Me*$_3$). Anal. Calcd for $C_{36}H_{57}N_2O_2Si_4Y$: C 57.58, H 7.66, N 3.73. Found: C 57.21, H 7.64, N 4.15.

(PCp*)Y[κ^2-(N,N)-iPrN(CH$_2$SiMe$_3$)CN(i-Pr)]$_2$ (5). Diisopropylcarbodiimide (60 mg, 0.5 mmol) ($Me_2CHNCNCHMe_2$) was added to 60 mg of **1** (0.1 mmol) in 1 mL of toluene solution and allowed to stir overnight. Removal of the toluene solvent under vacuum, followed by repeated washing with hexane and drying *in vacuo*, afforded an off-white powder quantitatively. ^{1}H NMR (C_6D_6, 300 MHz): δ 8.71 (d, $^3J_{HH}$ = 8.6 Hz, 2H, *1-aryl H*), 8.55 (d, $^3J_{HH}$ = 9.3 Hz, 2H, *4-aryl H*), 7.53 (t, $^3J_{HH}$ = 7.8 Hz, 2H, *2-arylH*), 7.37 (m, $^3J_{HH}$ = 7.6 Hz, 2H, *3-aryl H*), 3.26 (m, 4H, C*H*Me$_2$), 2.87 (s, 6H, Cp*Me*), 2.41 (s, 3H, Cp*Me*), 1.83 (s, 4H, *CH*$_2$SiMe$_3$), 0.94 (d, 24H, $^3J_{HH}$ = 7.6 Hz, CH*Me*$_2$) 0.06 (s, 18H, Si*Me*$_3$). ^{13}C NMR (75.5 MHz, C_6D_6): δ 177.40 (*NCN*), 127.06, 125.88, 124.35, 124.31 (*arylC*), 48.15 (*CH*Me$_2$), 25.91 (CH*Me*$_2$), 18.96 (*C*H$_2$SiMe$_3$), 17.22 (Cp*Me*$_2$), 13.20 (Cp*Me*), 0.42 (Si*Me*$_3$). Anal. Calcd for $C_{42}H_{67}N_4Si_2Y$: C 65.25, H 8.74, N 7.25. Found: C 64.42, H 8.25, N 6.51.

(PCp*)Y(CCSiMe$_3$)$_2$(THF) (6) and [PCp*Y(CCSiMe$_3$)(THF)]$_2$-(μ^2-CCSiMe$_3$)$_2$] (7). Trimethylsilylacetylene (20 mg, 0.2 mmol) was added to **1** (32 mg, 0.05 mmol) in a mixture of 0.5 mL of THF and 3 mL of toluene while stirring. The solution was allowed to stir overnight. Removal of solvent under reduced pressure gave 30 mg of **7** (characterized by NMR only) as a pale yellow residue. This solid was dissolved in hexanes and cooled at −40 °C to give **7** as nearly colorless plates. X-ray analysis showed that **7** is the acetylide-bridged dimer of **6** as a monotoluene solvate. Yield: 91%. Mp: 102 °C (dec). In solution, **7** reverts to the monomer **6** as evidenced by the doublet due to ^{89}Y coupling for the acetylide α-carbon. ^{1}H NMR (C_6D_6, 500 MHz): δ 8.78 (d, $^3J_{HH}$ = 8.0 Hz, 2H, *1-arylH*), 8.39 (d, $^3J_{HH}$ = 7.8 Hz, 2H, *4-arylH*), 7.50 (m, 2H, *2-arylH*), 7.32 (m, 2H, *3-arylH*), 3.26 (t, 4H, α-THF *CH*$_2$), 2.98 (s, 6H, Cp*Me*), 2.36 (s, 3H, Cp*Me*), 0.60 (brs, 4H, β-THF *CH*$_2$), 0.28 (s, 18H, Si*Me*$_3$). ^{13}C NMR (125.7 MHz, C_6D_6): δ 171.23 (d, $^1J_{YC}$ = 53.6 Hz, α-YC), 132.37, 129.84, 129.47, 127.34, 126.35, 124.68, 123.85, 120.27, 117.23 (*arylC*), 71.95, 25.45 (*THF*), 16.53 (Cp*Me*$_2$), 13.80 (Cp*Me*), 1.09 (Si*Me*$_3$), β-carbon of the acetylide was not observed. Anal. Calcd for **7**·toluene (matching the X-ray) $C_{75}H_{94}O_2Si_4Y_2$: C 68.37, H 7.20. Found: C 68.75, H 6.92.

Ethylene Polymerization by 1 Treated with Trityl Tetrakis(perfluorophenyl)borane. $[Ph_3C]^+[B(C_6F_5)_4]^-$ (15 mg, 0.016 mmol) in 1 mL of toluene was added to complex **1** (10 mg, 0.016 mmol) in 3 mL of toluene solution with rapid stirring. The color of the solution changed from pale yellow to red immediately and then slowly faded back to pale yellow after 2 h. The solution was exposed to vacuum for 20 s to remove the nitrogen gas from the flask, and ethylene gas, dried over 4 Å sieves, was introduced into the flask at 1 bar of pressure. After 30 min, the reaction mixture changed to a bright yellow color with formation of significant amounts of precipitate. Addition of methanol terminated the polymerization, and the color of solution and precipitate changed to white immediately. Removal of solvent, followed by washing with a methanolic HCl solution afforded 170 mg of polyethylene. The catalytic activity for polymerization of ethylene was estimated to be ca. 20 kg mol^{-1} h^{-1} bar^{-1} based on the molar amount of **1** used.

In separate NMR tube experiments, the ^{1}H and ^{19}F NMR of the species formed by addition of 1 equiv of $[Ph_3C]^+[B(C_6F_5)_4]^-$ to **1** in d_8-toluene and d_5-bromobenzene were examined at the red and yellow stages. In both solvents and at both stages, the spectra were extremely complicated and contained a very large number of resonances (^{1}H), many of which were broad (^{1}H and ^{19}F). The ^{1}H NMR spectra in the two solvents also differed significantly from one another. No assignments could be made for the species present in either solvent.

Table 1. Summary of Crystallographic Data for 1 and 7·toluene[a]

	1	**7**·toluene
formula	$C_{32}H_{47}OSi_2Y$	$C_{75}H_{94}O_2Si_4Y_2$
fw (g mol^{-1})	592.79	1317.68
cryst size (mm)	0.32 × 0.28 × 0.21	0.21 × 0.13 × 0.07
cryst color and habit	pale yellow prism	colorless plate
a (Å)	11.1359(5)	10.5591(12)
b (Å)	12.7246(6)	24.499(3)
c (Å)	12.9267(6)	27.461(3)
α (deg)	76.0030(10)	90
β (deg)	74.1890(10)	100.724(10)
γ (deg)	64.5570(10)	90
V (Å^3)	1574.97(13)	6979.7(13)
calc density (g cm^{-3})	1.250	1.254
space group	$P\bar{1}$ (No. 2)	$P2_1/c$ (No. 14)
Z	2	4
2θ range (deg)	1.79 - 27.5	1.51 – 25.25
*F*000	628	2776
linear abs coeff (mm^{-1})	1.949	1.767
no. of reflns measured	24 128	10 4015
no. of unique reflns	7233	12642
no. of params refined	334	764
no. of params restrained	0	15
R1[b], wR2[c]	0.0305, 0.0750	0.0425, 0.0849
R1[b], wR2[c] all data	0.0350, 0.0770	0.0662, 0.0926
GOF on F^2	1.049	1.030

[a] T = 86(2) K (**1**), 89(2) K (**7**) using Mo Kα (λ = 0.71073 Å). [b] $R = \sum(|F_o| - |F_c|)/\sum|F_o|$. [c] $R_w = [\sum w(|F_o| - |F_c|^2)/\sum w(|F_o|)^2]^{1/2}$.

X-ray Crystallographic Studies. Crystals of compound **1** or **7** (the latter as a monotoluene solvate) were removed from the flask and covered with a layer of hydrocarbon oil. A suitable crystal was selected, attached to a glass fiber, and placed in the low-temperature nitrogen stream.[10] Data for **1** and **7** were collected at 86(2) and 89(2) K, respectively, using a Bruker/Siemens SMART APEX instrument (Mo Kα radiation, λ = 0.71073 Å) equipped with a Cryocool NeverIce low-temperature device. Data were measured using omega scans of 0.3° per frame for 5 s, and a full sphere of data was collected. For **1**, a total of 2450 frames were collected with a final resolution of 0.77 Å; in the case of **7**, 2400 frames with a final resolution of 0.83 Å were collected. The first 50 frames were re-collected at the end of data collection to monitor for decay. Cell parameters were retrieved using SMART[11] software and refined using SAINTPlus[12] on all observed reflections. Data reduction and correction for *Lp* and decay were performed using the SAINTPlus software. Absorption corrections were applied using SADABS.[13] Both structures were solved by direct methods and refined by the least-squares method on F^2 using the SHELXTL program package.[14] The structure of **1** was solved in the space group $P\bar{1}$ (# 2) and that of **7** in the space group $P2_1/c$ (#14) by analysis of systematic absences. All atoms of **1** were refined anisotropically. In the case of **7**, one $SiMe_3$ group (C57, C58, C59) was disordered and modeled in two positions with occupancies of 40:60%. The disordered carbons were refined isotropically, while all other non-hydrogen atoms were refined anisotropically. Details of the data collection and refinement are given in Table 1. Further details are provided in the Supporting Information.

Results and Discussion

Synthesis and Characterization. The acid–base reaction between 1 equiv of PCp*H and $Y(CH_2SiMe_3)_3(THF)_2$ in

(10) Hope, H. *Prog. Inorg. Chem.* **1995**, *41*, 1.
(11) *SMART*: v.5.626, Bruker Molecular Analysis Research Tool: Bruker AXS: Madison, WI, 2002.
(12) *SAINTPlus*: v.6.36a, Data Reduction and Correction Program; Bruker AXS: Madison, WI, 2001.
(13) *SADABS*: v.2.01, An Empirical Absorption Correction Program; Bruker AXS: Madison, WI, 2001.
(14) Sheldrick, G. M. *SHEXTL*: v.6.10, Structure Determination Software Suite;Bruker AXS: Madison, WI, **2001**.

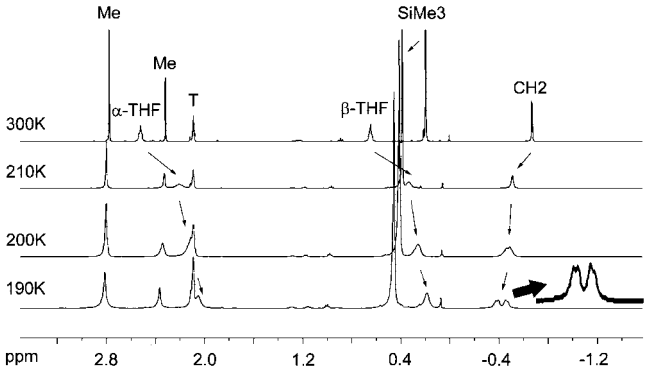

Figure 1. Variable-temperature ^{1}H NMR spectra (500 MHz, d_8-toluene (T)) spectra for the upfield region of **1**.

toluene at room temperature cleanly affords (PCp*)-$Y(CH_2SiMe_3)_2(THF)$ (**1**) as pale yellow prisms in 20% yield after recrystallization (eq 1). The low yield is mainly due to the extremely high solubility of **1** in hexane. Attempts to prepare a bis PCp* complex using 2 equiv of PCp*H resulted in formation of **1** and unreacted PCp*H according to ^{1}H NMR spectroscopy. This fact, and the observation that **1** is stable toward redistribution in solution over a period of weeks, suggests that the bis PCp* complex is too crowded to form by this route.

$$\mathrm{PCp^*H} + \mathrm{Y[CH_2SiMe_3]_3[THF]_2} \rightarrow \mathrm{(PCp^*)Y(CH_2SiMe_3)_2(THF)}\ (\mathbf{1}) + \mathrm{SiMe_4} \quad (1)$$

The ^{1}H NMR spectrum of **1** at 300 K in d_8-toluene shows a single doublet ($^2J_{YH} = 3.2$ Hz) at -0.60 ppm for the alkyl CH_2 resonance, consistent with average C_{2v} symmetry (Figure 1). The observation of high symmetry implies that rapid dissociation and reassociation of coordinated THF and rapid rotation about the PCp* centroid−yttrium bond is occurring at room temperature. The THF α- and β-protons appear as multiplets at 2.52 and 0.60 ppm, respectively. An upfield shift for the THF protons is expected on coordination, but the magnitude observed for **1** is probably due in part to the shielding effect of the phenanthrene π-system of the PCp* ligand.

The upfield region of the variable-temperature ^{1}H NMR spectra for **1** recorded between 300 and 190 K are shown in Figure 1. Two notable features are observed on cooling: (i) the THF resonances shift continuously upfield with decreasing temperature and (ii) the alkyl CH_2 resonance decoalesces from a doublet to a pair of doublets of doublets ($^2J_{HH} = 9.3$ Hz, $^2J_{YH} = 3$ Hz). The upfield shift of the THF resonances plotted in Figure 2 is consistent with a rapid equilibrium between **1** and its THF-free analogue **1′** (eq 2). The α-protons of free THF in d_8-toluene appear at 3.57 ppm, so it is clear that even at room temperature, **1** is present in significant concentration in solution. However, the fact that no resonances for free THF are observed at low temperature indicates that the THF exchange process remains rapid even at 190 K. A very rough estimate of the thermodynamic parameters for eq 2 can be obtained if we assume that the limiting (100% in the form of **1**) chemical shift for the α-THF protons is ca. 1.5 ppm. This value is a crude estimate based on the shifts observed for related bis PCp complexes that do not exchange

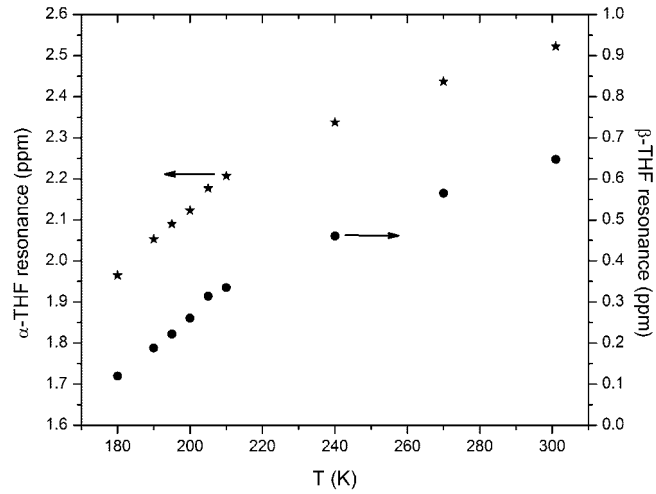

Figure 2. Chemical shift versus temperature plot for the THF resonances of **1**.

THF at room temperature.[15] Taking this value as 100% complex **1** and 3.57 ppm as 100% free THF, a van't Hoff plot for the equilibrium between **1** and **1′** shown in eq 2 can be constructed (Figure 3) that yields $\Delta H°$ and $\Delta S°$ values of 10.5 ± 0.5 kJ mol^{-1} and 36 ± 5 J mol^{-1} K^{-1}, respectively. These values are somewhat smaller than those observed by Okuda et al. for $[\{(C_5Me_4)SiMe_2N^tBu\}Y(CH_2SiMe_3)(THF)]$ ($\Delta H° = 24 \pm 3$ kJ mol^{-1}; $\Delta S° = 61 \pm 12$ J mol^{-1} K^{-1}),[15b] but they are consistent with THF dissociation.

In contrast to THF exchange, the process that renders the alkyl CH_2 resonances equivalent becomes slow on the NMR time scale at ca. 200 K (Figure 1), so that inequivalent CH_aH_b protons displaying geminal coupling (as well as coupling to ^{89}Y) are observed. The two alkyls remain equivalent to each other, indicating that the low-temperature symmetry has been reduced to C_s from C_{2v}. An Eyring plot (Figure 4) using rate constants derived from dynamic NMR simulations yields kinetic parameters of $\Delta H^‡$ and $\Delta S^‡$ of 43 ± 2 kJ mol^{-1} and 9 ± 5 J mol^{-1} K^{-1}, respectively.

Two explanations for the dynamic behavior of the CH_2 groups are possible depending on whether the THF-free complex **1′** has pyramidal or trigonal-planar geometry at the yttrium center (taking the Cp centroid to be one coordination site) in the ground state. If the ground state is pyramidal, then only inversion at Y would be required to make the protons of the CH_2 groups equivalent (Figure 5) assuming rapid rotation about the Y−PCp* bond. A planar ground state seems more likely for a d^0 metal center on the basis of steric considerations; however, previous *ab initio* and DFT calculations are divided on the preferred ground state.[16] Theoretical studies on Cp_2ScMe favored a planar

(15) The procedure used here is analogous to that in ref 15b, but unlike that case, stopped exchange between THF and **1′** was not observed even at low temperature, thus requiring estimation of the "100% coordinated" THF chemical shifts in order to estimate the mole fraction of **1**, **1′**, and THF present. This introduces additional uncertainty into estimation of $\Delta H°$ and especially $\Delta S°$, not included in the mathematical uncertainties quoted. The ln K vs $1/T$ plot showed some curvature at high temperatures (above 240 K), but the linear fit at low temperatures shown in Figure 3 is quite good, so we believe the assumptions made in estimating the "*100% coordinated*" THF chemical shifts are reasonable. The chemical shift of THF could also be influenced by differential anisotropic shielding for different rotamers in a slow Y−PCp* condition (similar to Figure 6); however, THF exchange must occur in order to achieve average C_{2v} symmetry at high temperature. The authors wish to thank one reviewer for helpful comments in interpretation of the dynamic behavior. (a) Sun, J. Ph.D. Thesis, University of Victoria, Victoria, B. C., Canada, 2007. (b) Hultzsch, K. C.; Spaniol, T. P.; Okuda, J. *Angew. Chem., Int. Ed. Engl.* **1999**, *38*, 227.

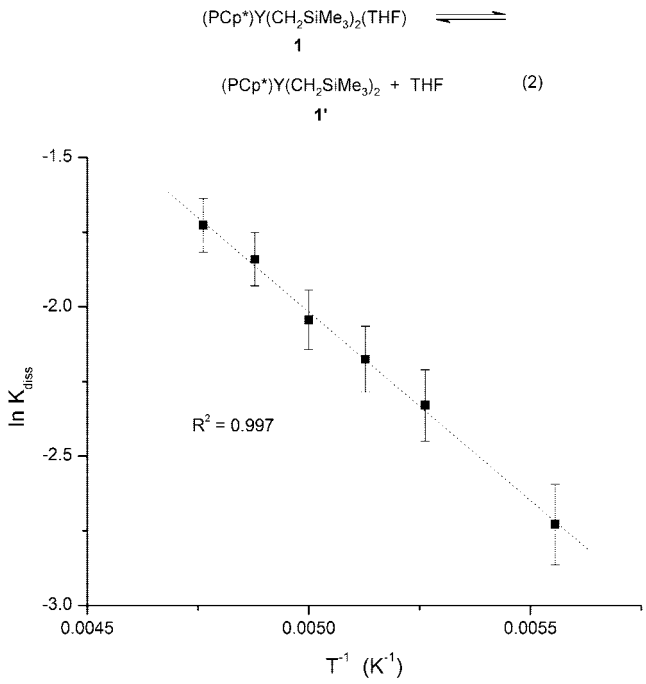

Figure 3. van't Hoff plot for the equilibrium between **1** and **1′** in d_8-toluene.

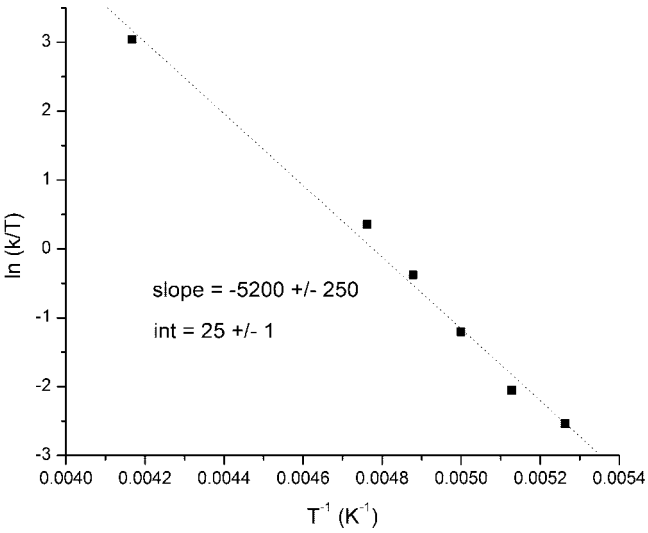

Figure 4. Eyring plot for the H_a/H_b exchange process of **1′** in d_8-toluene.

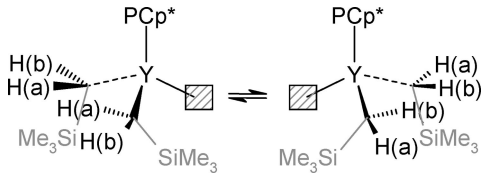

Figure 5. H(a)−H(b) exchange by pyramidal inversion at yttrium for **1′**.

ground state,[16a] but alkyls with β-hydrogens (Et, n-Pr) favored a pyramidal geometry to accommodate a β-CH agostic interaction.[16b,d] More recent work suggests that a pyramidal geometry is preferred in d^0 MX_3 systems when X is an alkyl due to some d orbital participation in the bonding.[16e] An agostic interaction between the α-CH_2 protons and the yttrium center,

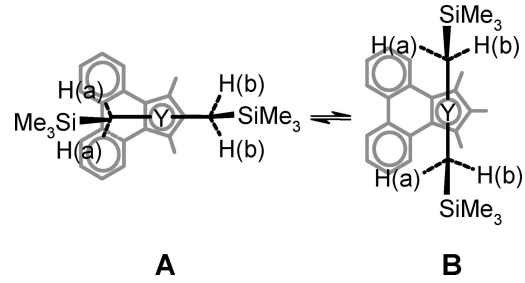

Figure 6. Two possible C_s symmetry rotamers for the ground state of **1′**.

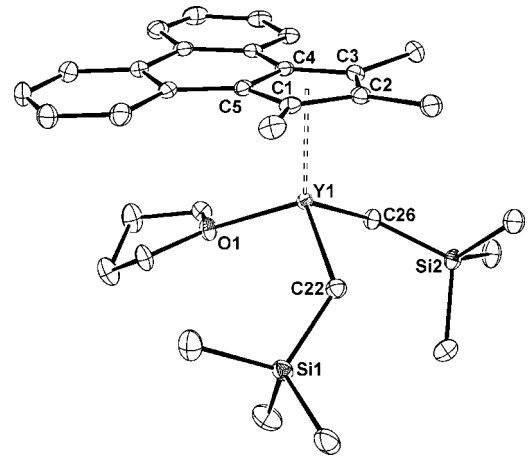

Figure 7. OTERP3[20] plot (40% probability ellipsoids) of **1**.

similar to that observed in Cp*La[$CH(SiMe_3)_2$]$_2$,[17] cannot be entirely ruled out in the base-free species **1′**; however, the $^{13}C-^{1}H$ coupling constant for the Y−CH_2 groups in **1** is 102 Hz and does not vary significantly with temperature, suggesting that agostic interactions are unlikely to be present in solution (or the solid state, see below). Interestingly, Casey[18] reported a very similar barrier to alkene dissociation and inversion ($\Delta G^{\ddagger}$ = 40 ± 1 kJ mol^{-1} at coalescence, T = 201 K) in the tethered alkene complex $(C_5Me_5)_2Y(\eta^1{:}\eta^2$-$CH_2CH_2CH(Me)CH{=}CH_2)$, lending credibility to slow inversion as the dynamic process at play here.

If a trigonal planar ground state is assumed, then all CH_2 protons remain equivalent if rapid rotation about the PCp*−yttrium centroid occurs. However, if rotation becomes slow on the NMR time scale, one of two C_s symmetry rotamers could become the ground state (Figure 6). In order to explain the observed inequivalence of protons on the same alkyl carbon but the equivalence of the two alkyl groups, rotamer **B** shown in Figure 6 must be the most stable geometry. This seems reasonable in that it places neither alkyl group directly under the phenanthrene or, perhaps more importantly, Cp* rings.

The solid-state structure of **1** determined by X-ray crystallography is shown in Figure 7; crystallographic data are summarized in Table 1, and selected bond distances and angles

(16) (a) Kawamura-Kuribayashi, H.; Koga, N.; Morokuma, K. *J. Am. Chem. Soc.* **1992**, *114*, 8687. (b) Ziegler, T.; Folga, E.; Berces, A. *J. Am. Chem. Soc.* **1993**, *115*, 638. (c) Woo, T. K.; Fan, L.; Ziegler, T. *Organometallics* **1994**, *13*, 2252. (d) Weiss, H.; Ehrig, M.; Ahlrichs, R. *J. Am. Chem. Soc.* **1994**, *116*, 4919. (e) Yoshida, T.; Koga, N.; Morokuma, K. *Organometallics* **1995**, *14*, 746. (f) Perrin, L.; Maron, L.; Eisenstein, O. *Faraday Discuss.* **2003**, *124*, 25.

(17) den Haan, K. H.; de Boer, J. L.; Teuben, J. H. *Organometallics* **1986**, *5*, 1726.

(18) Casey, C. P.; Fagan, M. A.; Hallenback, S. L. *Organometallics* **1998**, *17*, 287.

Table 2. Selected Bond Distances (Å) and Angles (deg) for 1[a]

Bond Distances			
Y(1)−C(1)	2.675(2)	Y(1)−C(2)	2.695(2)
Y(1)−C(3)	2.679(2)	Y(1)−C(4)	2.631(2)
Y(1)−C(5)	2.630(2)	Y(1)−Cp1	2.370
Y(1)−C(22)	2.390(2)	Y(1)−C(26)	2.383(2)
Y(1)−O(1)	2.3239(12)		
Bond Angles			
Cp1−Y(1)−C(22)	116.0	Cp1−Y(1)−C(26)	138.6
Cp1−Y(1)−O(1)	115.1	C(22)−Y(1)−C(26)	107.75(6)
C(22)−Y(1)−O(1)	93.30(5)	C(26)−Y(1)−O(1)	112.10(5)
Y(1)−C(22)−Si(1)	123.76(9)	Y(1)−C(26)−Si(2)	125.92(9)

[a] Estimated standard deviation in parentheses; Cp^1 is the centroid of C(1)−C(5).

are given in Table 2. Complex **1** adopts a pseudotetrahedral, three-legged piano stool geometry in the solid state. From the bond lengths within the PCp* ligand itself, it is apparent that to a certain extent this ligand can be viewed as three isolated 6π-electron systems: C1−C5 of the Cp unit (mean C−C bond length = 1.425 Å) and C6−C11 and C12−C17 of the benzenoid rings (mean C−C = 1.398 and 1.397 Å, respectively) with longer distances between these rings (C4−C17, 1.452(2) Å; C5−C6, 1.452(2) Å; C11−C12, 1.473(3) Å). The Y−C distances to the Cp ring fall into two distinct groups with the shorter set of contacts between Y and the phenanthrene ring fusion carbons (Y1−C4, 2.631(2) and Y1−C5, 2.630(2) Å) and the longer set to the three carbons bearing the methyl groups (Y1−C1, 2.675(2); Y1−C2, 2.695(2); Y1−C3, 2.679(2) Å). While these differences are small, they are significant and the opposite of the pattern usually observed in yttrium indenyl systems.[19] The most obvious explanation for this fact is that the methyl groups represent more steric bulk than does the phenanthrene ring and the yttrium moves toward the less crowded edge of the Cp ring. Overall, the Y−Cp C and Y−O distances in **1** are quite similar to other six-coordinate Y complexes (Y−C_{ring}: range 2.618–2.698 Å, median 2.627 Å; Y−O range: 2.299–2.372 Å, median 2.338 Å).[21] The Y−alkyl C distances are among the shortest reported in six-coordinate Y-alkyls (Y−C_{alkyl}: range 2.388–2.524 Å median 2.450 Å).[21] The closest Y−-H contacts of 2.819 Å are to H22A and H22B on C22. The long Y−H distance and the normal Y1−C22−Si1 angle (123.76(9)°) rule out the presence of an α-agostic interaction in this complex.

Reactivity Studies. Complex **1** reacts with 2,2′-bipyridine (bipy) in toluene to form the four-legged piano stool complex PCp*Y(CH_2SiMe_3)$_2$(bipy) (**2**) as a red solid (Scheme 1). Unlike, THF-adduct **1**, **2** does not undergo ligand exchange on the NMR time scale with free bipy in solution. Direct reaction of Y(CH_2SiMe_3)$_3$(THF)$_2$ with PCp*H in the presence of bipy affords **2** in excellent yield. This greater ease of access makes **2** a more desirable starting material than **1**, but this fact was realized after most of the reaction chemistry described below

Scheme 1

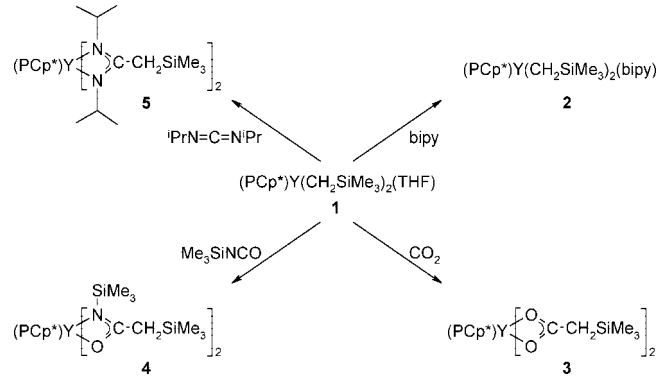

was completed, so the initial chemistry was carried out using the harder to prepare **1**.

Complex **1** undergoes clean 1,2-insertion of CO_2, Me_3SiNCO, or $^iPrN{=}C{=}N^iPr$ into both yttrium−alkyl bonds to form the bis carboxylate (**3**), amidate (**4**) and amidinate (**5**) complexes (Scheme 1). In each case, the most notable evidence for insertion is the disappearance of the upfield CH_2 doublet of **1** and the appearance of a downfield singlet at 1.10 (**3**), 1.65 (**4**), or 1.83 (**5**) ppm. Similarly, all three complexes show a characteristic downfield ^{13}C resonance due to the central C of the carboxylate (δ 185.42), amidate (δ 188.54), or amidinate (177.40) ligands.[22] *Cis* and *trans* isomers are possible for the amidate complex (**4**), but a single CH_2 resonance is observed for all four protons of the CH_2SiMe_3 groups bonded to the central carbon. This is significant because the CH_2 resonances of *either* the *cis* or *trans* isomers of **4** should be inequivalent by symmetry. A dynamic process involving a $\kappa^2 \rightarrow \kappa^1$ rearrangement of the amidate ligand, most likely via N dissociation, followed by rotation about the Y−O and C(O)−CH_2 bonds would interconvert the *cis* and *trans* isomers and render the CH_2 protons equivalent (Figure 8). The crystals of these complexes lose solvent very rapidly, and we have been unable to obtain X-ray structural data, so we cannot rule out the possibility that **3**−**5** contain bridging ligands in a dimeric (or higher array). However, if this is the case, the bridged structures must also be undergoing rapid fluxional processes to explain the simple spectra obtained.

Complex **1** undergoes an acid–base (protonolysis) reaction with trimethylsilylacetylene to afford a bis(acetylide) complex. In solution, this product (**6**) shows clear NMR evidence for terminal acetylide ligation, as shown by the simple doublet due to $^{89}Y-^{13}C$ coupling for the α-acetylide carbon resonance (δ 171.2, $^1J_{YC}$ = 55.5 Hz). Crystallization of **6** from a mixture of

(19) (a) Gavenonis, J.; Tilley, T. D. *J. Organomet. Chem.* **2004**, *689*, 870. (b) Qi, M.; Shen, Q.; Chen, X.; Weng, L.-H. *Yingyong Huaxue (Chin. J. Appl. Chem.)* **2003**, *20*, 629. (c) Kretschmer, W. P.; Troyanov, S. I.; Meetsma, A.; Hessen, B.; Teuben, J. H. *Organometallics* **1998**, *17*, 284.

(20) Farrugia, L. J. ORTEP3 for Windows. *J. Appl. Crystallogr.* **1997**, *30*, 565.

(21) (a) Evans, W. J.; Boyle, T. J.; Ziller, J. W. *Organometallics* **1993**, *12*, 3998. (b) Arndt, S.; Trifonov, A.; Spaniol, T. P.; Okuda, J.; Kitamura, M.; Takahashi, T. *J. Organomet. Chem.* **2002**, *647*, 158. (c) Gendron, R. A. L.; Berg, D. J.; Barclay, T. *Can. J. Chem.* **2002**, *80*, 1285. (d) Roesky, P. W. *Organometallics* **2002**, *21*, 4756. (e) Trifonov, A.; Spaniol, T. P.; Okuda, J. *J. Chem. Soc., Dalton Trans.* **2004**, 2245. (f) Trifonov, A.; Spaniol, T. P.; Okuda, J. *Organometallics* **2001**, *20*, 4869. (g) Hultzch, K. C.; Voth, P.; Becherle, K.; Spaniol, T. P.; Okuda, J. *Organometallics* **2000**, *19*, 228.

(22) (a) Djordjevic, C.; Gonshor, L. G.; Schiavelli, M. D.; Angevine-Malley, L. S. *J. Less Common Met.* **1983**, *94*, 355. (b) Power, M. B.; Bott, S. G.; Clark, D. L.; Atwood, J. L.; Baron, A. L. *Organometallics* **1990**, *9*, 3086. (c) Bambirra, S.; Brandsma, M. J. R.; Brussee, E. A. C.; Meetsma, A.; Hessen, B.; Teuben, J. H. *Organometallics* **2000**, *19*, 3197. (d) Zhang, J.; Ruan, R.; Shao, Z.; Cai, R.; Weng, L.; Zhou, X. *Organometallics* **2002**, *21*, 1420. (e) Zhou, X. G.; Zhang, L. B.; Zhu, M.; Cai, R. F.; Weng, L. H. *Organometallics* **2001**, *20*, 5700. (f) Haan, K. H.; Luinstra, A.; Meetsma, A.; Teuben, J. H. *Organometallics* **1987**, *6*, 1509. (g) Schumann, H.; Meese-Marktscheffel, J. A.; Dietrich, A.; Görlitz, F. H. *J. Organomet. Chem.* **1992**, *430*, 299.

(23) (a) Reversible coupling: Lee, L.; Berg, D. J.; Bushnell, G. W. *Organometallics* **1995**, *14*, 5021. (b) Heeres, H. J.; Teuben, J. H. *Organometallics* **1991**, *10*, 1980. (c) Heeres, H. J.; Nijhoff, J.; Teueben, J. H. Rogers, R. D. *Organometallics* **1993**, *12*, 2609. (d) Cameron, T. C.; Gordon, J. C.; Scott, B. L. *Organometallics* **2004**, *23*, 2995. Irreversible coupling. (e) Evans, W. J.; Keyer, R. A.; Zhang, H.; Atwood, J. L. *J. Chem. Soc., Chem. Commun.* **1987**, *837*. (f) Evans, W. J.; Keyer, R. A.; Ziller, J. W. *Organometallics* **1990**, *9*, 2628. (g) Evans, W. J.; Keyer, R. A.; Ziller, J. W. *Organometallics* **1993**, *12*, 2618. (h) Forsyth, C. M.; Nolan, S. P.; Stern, C. L. Marks, T. J.; Rheingold, A. L. *Organometallics* **1993**, *12*, 3618.

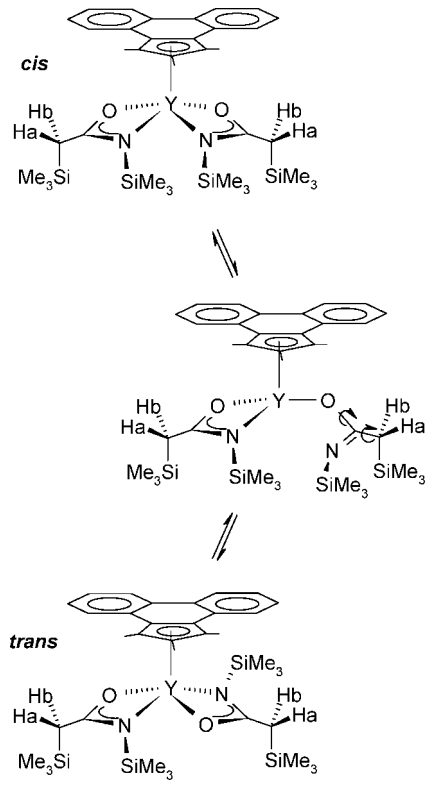

Figure 8. Rapid *cis*−*trans* isomerization of **4**.

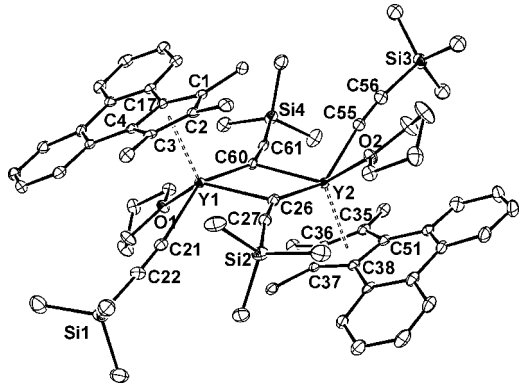

Figure 9. OTERP3[20] plot (40% probability ellipsoids) of **7**·toluene. Toluene of solvation omitted for clarity.

toluene and hexane afforded colorless crystals that proved to be the acetylide -bridged dimer **7** by X-ray crystallography. These crystals produce the characteristic signals of **6** when redissolved in d_6-benzene, indicating that **6** and **7** readily interconvert (eq 3). Interestingly, although we have previously observed reversible formation of a coupled butatrienediyl unit from bridging acetylides in Y(DAC)(CCPh) (DAC = 4,13-diaza-18-crown-6)[23a] and others have reported similar results in Cp-based systems,[23b,h] **7** shows no tendency to couple. The factors that govern the coupling of acetylides to butatrienediyls have not been established, but it is clear that no one ligand set promotes this reaction.

$$2(PCp^*)Y(CCSiMe_3)_2(THF)(\mathbf{6}) \rightleftharpoons [(PCp^*)Y(CCSiMe_3)(THF)]_2[\mu\text{-}CCSiMe_3]_2(\mathbf{7}) \quad (3)$$

The crystal structure of dimer **7** is shown in Figure 9; crystallographic data are summarized in Table 1, and selected bond distances and angles are collected in Table 3. The acetylide bridges in **7** are highly asymmetric, tilting strongly toward one

Table 3. Selected Bond Distances (Å) and Angles (deg) for 7·toluene[a]

Bond Distances			
Y(1)−C(1)	2.670(3)	Y(1)−C(2)	2.713(3)
Y(1)−C(3)	2.693(3)	Y(1)−C(4)	2.637(3)
Y(1)−C(17)	2.657(3)	Y(1)−Cp[1]	2.388
Y(1)−C(21)	2.412(3)	Y(1)−C(26)	2.507(3)
Y(1)−C(60)	2.521(3)	Y(1)−O(1)	2.361(2)
Y(2)−C(35)	2.698(3)	Y(2)−C(36)	2.718(3)
Y(2)−C(37)	2.672(3)	Y(2)−C(38)	2.663(3)
Y(2)−C(51)	2.634(3)	Y(2)−Cp[2]	2.384
Y(2)−C(26)	2.517(3)	Y(2)−C(55)	2.397(3)
Y(2)−C(60)	2.499(3)	Y(2)−O(2)	2.380(2)
Bond Angles			
Cp[1]−Y(1)−C(21)	106.9	Cp[1]−Y(1)−C(26)	111.0
Cp[1]−Y(1)−C(60)	108.9	Cp[1]−Y(1)−O(1)	111.5
C(21)−Y(1)−C(26)	93.12(10)	C(21)−Y(1)−C(60)	143.83(10)
C(21)−Y(1)−O(1)	83.78(8)	C(26)−Y(1)−C(60)	78.94(10)
C(26)−Y(1)−O(1)	136.37(8)	C(60)−Y(1)−O(1)	78.57(8)
Cp[2]−Y(2)−C(26)	108.5	Cp[2]−Y(2)−C(55)	109.2
Cp[2]−Y(2)−C(60)	109.4	Cp[2]−Y(2)−O(2)	113.8
C(26)−Y(2)−C(55)	142.03(10)	C(26)−Y(2)−C(60)	79.17(10)
C(26)−Y(2)−O(2)	79.83(8)	C(55)−Y(2)−C(60)	92.76(10)
C(55)−Y(2)−O(2)	80.97(9)	C(60)−Y(2)−O(2)	136.06(9)
Y(1)−C(21)−C(22)	171.9(3)	Y(1)−C(26)−C(27)	105.8(2)
Y(1)−C(60)−C(61)	154.9(2)	Y(1)−C(26)−Y(2)	100.85(10)
Y(1)−C(60)−Y(2)	100.98(11)	Y(2)−C(26)−C(27)	151.2(2)
Y(2)−C(55)−C(56)	171.6(3)	Y(2)−C(60)−C(61)	154.9(2)

[a] Estimated standard deviation in parentheses; Cp[1] and Cp[2] are the centroids of C(1)−C(2)−C(3)−C(4)−C(17) and C(35)−C(36)−C(37)−C(38)−C(51), respectively.

Y center, as noted by the widely divergent Y−C_α−C_β angles (Y1−C26−C27, 105.8(2)° and Y2−C26−C27, 151.2(2)°, $\Delta\varphi$ = (large M−C_α−C_β)−(small M−C_α−C_β) = 45.4°; Y2−C60−C61, 102.2(2)° and Y1−C60−C61, 154.9(2)°, $\Delta\varphi$ = 52.7°). Despite this fact, the closest Y−C_β distance is just over 3 Å, and there is no statistically significant difference between the C−C triple bond distance for the bridging (mean C−C 1.224 Å) and terminal acetylides (mean C−C 1.218 Å). In addition, the asymmetry of the bridging acetylide angles is not reflected in the corresponding Y−C_α distances (Y1−C26, 2.507(3); Y2−C26, 2.517(3); Y1−C60, 2.521(3); Y2−C60, 2.499(3) Å). A survey of all lanthanide and group 3 bridging acetylides shows that the asymmetry in bridge angles is in the range $\Delta\varphi$ = 2.3–65.8° with no clear relationship between the degree of asymmetry and the Y−C_α distances.[23a,24] In fact, one structure consisting of two independent molecules displays widely divergent $\Delta\varphi$ angles of 2.3° and 61.0° for the same compound.[24f] From this we conclude that solid-state packing forces probably play a major role in bridge angle asymmetry ($\Delta\varphi$), and any π-interactions between the alkynyl group and the metal are weak.

As commonly observed,[24e] the bridging Y−C_α distances are much longer than the terminal distances (mean Y−C_α bridge, 2.511; mean Y−C_α terminal, 2.405 Å). As in **1**, the bonding between Y and the PCp* ring is slipped somewhat so that Y is

(24) (a) Atwood, J. L.; Hunter, W. E.; Wayda, A. L.; Evans, W. J. *Inorg. Chem.* **1981**, *20*, 4115. (b) Evans, W. J.; Bloom, I.; Hunter, W. E.; Atwood, J. L. *Organometallics* **1983**, *2*, 709. (c) Boncella, J. M.; Tilley, T. D.; Andersen, R. A. *J. Chem. Soc., Chem. Commun.* **1984**, 710. (d) Zhang, S.; Zhuang, X.; Zhang, J.; Chen, W.; Liu, J. *J. Organomet. Chem.* **1999**, *584*, 135. (e) Tazelaar, C. G. J.; Bambirra, S.; van Leusen, D.; Meetsma, A.; Hessen, B.; Teuben, J. H. *Organometallics* **2004**, *23*, 936. (f) Forsyth, C. M.; Deacon, G. B.; Field, L. D.; Jones, C.; Junk, P. C.; Kay, D. L.; Masters, A. F.; Richards, A. F. *J. Chem. Soc., Chem. Commun.* **2006**, 1003. (g) Federova, E. A.; Glushkova, N. M.; Bochkarev, M. N.; Shuman, G.; Khemling, K. *Russ. Chem. Bull.* **1996**, 2201. (h) Shen, Q.; Zheng, D.; Lin, L.; Lin, Y. *J. Organomet. Chem.* **1990**, *391*, 307. (i) Ren, J.; Hu, J.; Lin, Y.; Xing, Y.; Shen, Q. *Polyhedron* **1996**, *15*, 2165. (j) Nishiura, M.; Hou, Z.; Wakatsuki, Y.; Yamaki, T.; Miyamoto, T. *J. Am. Chem. Soc.* **2003**, *125*, 1184. (k) Duchateau, R.; van Wee, C. T.; Meetsma, A.; Teuben, J. H. *J. Am. Chem. Soc.* **1993**, *115*, 4931.

closest to the phenanthrene ring fusion carbons and furthest from the three PCp* carbons bearing the methyl groups. The amount of this distortion is 0.05Å in both **1** and **7**. Although **7** is formally seven-coordinate, the Y−C distances to the PCp* ligand are not significantly different from those in six-coordinate **1**, presumably reflecting the fact that the acetylides are small, rigid rod-like ligands that take up less space than a typical ligand.

Reaction with Ethylene. Complex **1** does not react with ethylene gas (5 atm) on its own; however, treatment with Ph_3C^+ $[B(C_6F_5)_4]^-$ in toluene yields a species that polymerizes ethylene at a modest rate (20 kg polyethylene mol $[Y]^{-1}$ h^{-1} bar^{-1}) at room temperature. The pale yellow solution of **1** immediately turns deep red on addition of Ph_3C^+ $[B(C_6F_5)_4]^-$, but this red solution produces no polymer formation in the first 90 min. The red color of the solution slowly fades to pale yellow over a period of ca. 2 h, at which point, ethylene polymerization initiates at the above rate. The ^1H and ^{19}F NMR spectra of the mixtures in d_8-THF or d_5-bromobenzene at the red and pale yellow stages are extremely complicated, so we cannot state with any certainty what the active catalytic species is. It would be logical to assume that an alkyl cation such as $[(PCp^*)Y(CH_2SiMe_3)]^+[B(C_6F_5)_4]^-$ forms, but this was not established from the spectroscopy at hand.[25]

We have established that PCp* is a viable ligand in yttrium chemistry and provides access to robust mono(ligand) complexes that undergo donor substitution and insertion chemistry without PCp* loss or ligand redistribution. At this point, high solubility limits the yield of high-purity **1**, making more extensive investigation of its chemistry difficult. Less soluble analogues such as **2** should make access to large quantities more practical.

Acknowledgment. D.J.B. (Discovery Grant) gratefully acknowledges the support of the Natural Sciences and Engineering Research Council of Canada.

Supporting Information Available: Tables of atomic coordinates, bond distances, and angles, and anisotropic thermal parameters for **1** and **7** are available free of charge via the Internet at http://pubs.acs.org.

OM7007343

(25) (a) Related mono(ligand) lanthanide alkyl cations have been prepared that show significantly greater ethylene polymerization activity: Bambirra, S.; Otten, E.; van Leusen, D.; Meetsma, A.; Hessen, B. *Z. Anorg. Allg. Chem.* **2006**, *632*, 1950. (b) Bambirra, S.; Bouwkamp, M. W.; Meetsma, A.; Hessen, B. *J. Am. Chem. Soc.* **2004**, *126*, 9182. (c) Bambirra, S.; van Leusen, D.; Meetsma, A.; Hessen, B.; Teuben, J. H. *J. Chem. Soc., Chem. Commun.* **2003**, 522. (d) Bambirra, S.; van Leusen, D.; Meetsma, A.; Hessen, B. Z.; Teuben, J. H. *J. Chem. Soc., Chem. Commun.* **2001**, 637. (e) Hayes, P. G.; Piers, W. E.; McDonald, R. *J. Am. Chem. Soc.* **2002**, *124*, 2132. (f) Arndt, S.; Spaniol, T. P.; Okuda, J. *Organometallics* **2003**, *22*, 775. (g) Nakajima, Y.; Okuda, J. *Organometallics* **2007**, *26*, 1270, and references therein.